

HIGH RESOLUTION TARGET RANGE ESTIMATION USING FREQUENCY-STEPPED CW RADAR

G. A. Ybarra*, G. L. Bilbro**, S. M. Wu**, S. H. Ardalan**, C. P. Hearn***, and R. T. Neece***

* Duke University Dept. of Electrical Engineering, Durham, NC

** North Carolina State University, Dept. of Electrical and Computer Engineering, Raleigh, NC

*** NASA Langley Research Center, Hampton, VA

Abstract

An optimal signal processing algorithm is derived for obtaining high resolution target range estimates from a small set of narrow bandwidth frequency-stepped CW radar measurements. Performance of the optimization approach is illustrated using measured data obtained from an HP-8510 network analyzer.

Introduction

The physical data measured by a frequency-stepped CW radar system is a sequence of complex reflection coefficients as seen from the aperture plane to which the system is calibrated. The sequence of measured reflection coefficients may be interpreted as samples of the radar channel frequency response. Given these measurements, the objective is to determine the target range. The standard approach [1] is to perform an IFFT (Inverse Fast Fourier Transform) which produces an estimate of the radar channel time domain impulse response. Peaks in the impulse response correspond to reflections and their time delay corresponds to the target range. The resolution of this approach is limited by the measurement bandwidth. In certain applications, such as re-entry plasma density measurement [2,3], the bandwidth must be kept small. The resolution offered by the IFFT approach is often unsatisfactory and an alternative approach is required.

This paper presents the derivation of a new optimal signal processing algorithm which maximizes the range resolution obtainable from any set of frequency-stepped CW measurements. The derivation is general in the number of echoes, and a constant frequency interval between the measurement samples is not required. However, in order to illustrate the performance of the new optimal processing algorithm through its geometric interpretation, the specific problem of resolving the time delay between the first two echoes is addressed. It is shown that the optimization process can be interpreted as scanning a non-linear objective function surface using an organized procedure to find its absolute minimum. In the two reflection problem, the objective function surface is 3-dimensional allowing visual inspection. By visually examining the structural changes in these 3-D surfaces as measurement parameters are changed, insight into the underlying physical process becomes available at a glance.

The resolution achievable using the new optimization algorithm is demonstrated using measurements taken from an HP-8510 network analyzer. The first set of measurements was taken at the input port of an air-line coaxial standard containing two step discontinuities in characteristic impedance. The remainder of the measurements were taken at the input port of a microwave reflectometer test apparatus. The results of the optimization approach are compared to those produced by the conventional Inverse Fast Fourier Transform (IFFT) technique. The comparison shows that when the bandwidth is reduced far beyond the point at which the IFFT fails to distinguish two reflections that are known to exist, the optimization approach is able to clearly resolve the reflections and estimate the range to each source of reflection accurately.

Derivation

The optimization procedure minimizes the objective function

$$J = \sum_{i=1}^n |H(j(\omega_0 + i\Delta\omega)) - H_m(j(\omega_0 + i\Delta\omega))|^2 \quad (1)$$

where the $H_m(j(\omega_0 + i\Delta\omega))$ are the measured complex reflection coefficient pairs, the $H(j(\omega_0 + i\Delta\omega))$ are the values of the theoretical model, and i is the index number of each measurement which spans the integer range from 1-n. J is a function of the echo amplitudes A_i and delays t_i of the physical model

$$h(t) = A_1 \delta(t-t_1) + A_2 \delta(t-t_2) + A_3 \delta(t-t_3) + \dots \quad (2a)$$

$$H(j\omega) = A_1 e^{-j\omega t_1} + A_2 e^{-j\omega t_2} + A_3 e^{-j\omega t_3} + \dots \quad (2b)$$

Samples of this frequency response form the model values comprising $H(j(\omega_0 + i\Delta\omega))$ in (1). The objective is to find the global minimum of the performance metric (1) with respect to the amplitude-delay pairs A_i, t_i in the model (2). The highly non-linear metric (1) is minimized by iteratively solving the linear portion of the problem. The metric (1) is quadratic in the amplitude parameters A_i . This allows the A_i to be calculated in closed form by solving the least squares (LS) problem

$$Fa = f \quad (3)$$

where the complex ($n \times N$) matrix F is composed of frequency response estimates based on the model (2) and the complex vector f is composed of the physical frequency response measurements given by

$$f = [H_m(\omega_1) \ H_m(\omega_2) \ H_m(\omega_3) \ \dots \ H_m(\omega_n)]^T \quad (4)$$

The vector a in (3) contains the set of real amplitudes A_i to be determined

$$a = [A_1 \ A_2 \ A_3 \ \dots \ A_N]^T \quad (5)$$

The LS problem (3) is somewhat unusual since the matrix F and vector f are complex while the amplitude vector a is real. The solution to (3) is found by minimizing the real scalar that results from the following squared inner product.

$$y = \| (F_r + jF_i)a - (f_r + jf_i) \|^2 \quad (6)$$

$$y = (F_r a - f_r)^T (F_r a - f_r) + (F_i a - f_i)^T (F_i a - f_i) \quad (7)$$

$$y = a^T [F_r^T F_r + F_i^T F_i] a - a^T [F_r^T f_r + F_i^T f_i] - [f_r^T F_r + f_i^T F_i] a + f_r^T f_r + f_i^T f_i \quad (8)$$

where the subscripts r and i denote real and imaginary parts respectively. In order to minimize y , the gradient of (8) is taken with respect to the real amplitude vector a and set equal to the zero vector.

$$\frac{\partial y}{\partial a} = 0 = 2[F_r^T F_r + F_i^T F_i]a - 2[F_r^T f_r + F_i^T f_i] \quad (9)$$

The result of the minimization of (6) is a real, square set of linear equations.

$$[F_r^T F_r + F_i^T F_i]a = [F_r^T f_r + F_i^T f_i] \quad (10)$$

OF1

Solution of the least squares problem (3) requires assuming a set of delays t_i . The following optimization procedure may be followed for extracting the A_i, t_i pairs:

- 1) Choose the number N of A_i, t_i pairs to be determined.
- 2) Assume a sequence of t_i values and search for the global minimum of (1).

A grid search procedure for finding the global minimum of (1) is described in detail and illustrated in the next section.

Experimental results

The first data set used to illustrate the performance of the optimization technique is a sequence of reflection coefficients measured at the input port of the 7 mm Beatty Standard [4] which is shown in figure 1 along with its theoretical bounce diagram. The resulting time domain impulse responses for two measurement bandwidths obtained from the internal computer of an HP-8510 network analyzer are shown in figures 2 and 3. When the measurement bandwidth is reduced from 18 GHz to 2 GHz the IFFT approach clearly fails to resolve two distinct reflections that are known to exist. The optimal processing algorithm applied to both cases is equivalent to scanning the surfaces shown in figures 4 and 5. The global (absolute) minima of the objective functions shown in figures 4 and 5 correspond to the optimal time delays to the first two reflections. The objective function shown in figure 5 has a single global minimum. This global minimum can be found with little computation using a procedure called grid search: t_2 is held constant while the minimum of J is found along the t_1 dimension. Then, t_1 is held constant at the value previously found while the minimum of J is found along the t_2 dimension. This procedure is repeated until the time delay values are no longer updated. The global minimum in figure 5 may be found in two iterations of grid search, independent of initialization. The grooves in the surface which are aligned with the delay axes provide an easily scanned search path.

The second set of data consists of measurements of the reflection coefficient as seen from the input port of a rectangular waveguide feeding a circular horn antenna as shown in figure 6. This test apparatus was constructed at NASA Langley Research Center for the development of an electron plasma density profile measurement system to be flown aboard the space shuttle. The target range for this system is defined to be the distance from the center of the quartz glass interferer to the metal plate target. Figure 7 shows the IFFT of 801 measurements over a 4 GHz bandwidth. The amplitude optimized objective function using the same measurement parameters is shown in figure 8. The IFFT performed well for this case because the bandwidth (4 GHz) was large enough to provide the resolution needed to distinguish the interferer (quartz glass) from the metal plate target. If the number of measurements is reduced to 101 and the bandwidth to 500 MHz, the corresponding IFFT is shown in figure 9. The IFFT is marginally able to distinguish the two sources of reflection. In addition, the time delay estimates contain significant error. The objective function for this case is shown in figure 10. The global minima corresponding to the optimal delay pair (3.45 ns, 5.42 ns) are clearly separated which indicates enhanced resolution.

If the target range is reduced from 12.125" to 2.375" while holding the bandwidth constant (500 MHz) and the number of measurements constant (101), the resulting IFFT is shown in figure 11 and the corresponding objective function in figure 12. The theoretical time delay from the interfering quartz glass to the metal plate target is 0.422 ns. While the resulting IFFT is meaningless for this case due to the narrow measurement bandwidth, the optimization approach is still able to recover the target range with very high accuracy (0.420 ns). This final result is intended to show the limitation of the optimization approach.

Conclusion

This paper has presented the derivation and demonstration of a new algorithm for processing radar data produced by any frequency-stepped CW system. The derivation is based on minimizing the two-norm of the difference between the sequence of measured reflection coefficients and those produced by a model which assumes that the echoes from the radar channel are impulses in the time domain. A performance comparison between the IFFT and optimal processing techniques was presented in the context of two physical measurement sets. In the first set, the Beatty standard was terminated in a matched load and driven by an HP-8510 network analyzer. The measurement bandwidth was reduced from 18 GHz to

2 GHz and it was shown that while the IFFT produced meaningless reflection range estimates in the 2 GHz case, the optimal processing approach was able to clearly resolve the reflections and the resulting reflection range estimates were as accurate using 2 GHz bandwidth as those produced by the IFFT using 18 GHz. In the second set of measurements, a microwave reflectometer test apparatus, also driven by an HP-8510 network analyzer, was used to illustrate the effects of reducing the bandwidth, number of measurements, and target range on both the IFFT and optimization results. First, the metal plate target was set at a range of 12" and 801 measurements spanning a total bandwidth of 4 GHz were analyzed using both the IFFT and optimal processing algorithms. The target range estimates resulting from both methods were of equal accuracy. Then, the number of measurements was reduced from 801 to 101 and the bandwidth reduced to 500 MHz. Finally, the target was set to a range of 2.25", holding the number of measurements and bandwidth at 101 and 500 MHz respectively. The range resolution and accuracy deterioration produced by IFFT processing was clearly evident. However, the optimal processing approach could not only resolve the two reflections but could estimate both of their ranges with high accuracy. This result demonstrates the resolution enhancement offered by the optimal processing approach over IFFT processing.

Future research will be directed toward quantifying the amplitude and frequency of the perturbations that occur in the objective function surface as the bandwidth, or the number of measurements, is reduced. The number of delay dimensions will be increased and other search procedures investigated for efficient global minimum scanning.

References

- [1] *HP 8510 Network Analyzer Operating and Programming Manual*, Hewlett-Packard Company, Santa Rosa, CA, 1984.
- [2] G.A. Ybarra, S.H. Ardalan, C.P. Hearn, R.E. Marshall, and R.T. Neece, "Detection of Target Distance in the Presence of an Interfering Reflection Using a Double Side-Band Suppressed Carrier Microwave Radar System," *IEEE Transactions on Microwave Theory and Techniques*, May, 1991.
- [3] G.A. Ybarra, *High Resolution Target Range Estimation in Inhomogeneous Media using Millimeterwave Radar*, Ph.D. Dissertation, 1992.
- [4] R.W. Beatty, "Calculated and Measured S11, S21, and Group Delay for Simple Types of Coaxial and Rectangular Waveguide 2-Port Standards," *National Bureau of Standards Technical Note 657*, U.S. Department of Commerce, December 1974.
- [5] G.H. Golub, and C.F. Van Loan, *Matrix Computations*, Johns Hopkins University Press, Baltimore MD, 1989.
- [6] C.L. Lawson, and R.J. Hanson, *Solving Least Squares Problems*, Prentice-Hall, 1974.
- [7] Artech House, *Techniques of Radar Reflectivity Measurement*, Norwood, MA, 1984.
- [8] Artech House, *Principles and Applications of Millimeterwave Radar*, Norwood, MA, 1987.
- [9] G.J. Bird, *Radar Precision and Resolution*, Wiley, NY.
- [10] D.R. Wehner, *High Resolution Radar*, Artech House, Norwood, MA, 1987.
- [11] Z.A. Maricevic et al., "Time-Domain Measurements with the Hewlett-Packard Network Analyzer HP-8510 Using the Matrix Pencil Method," *IEEE Transactions on Microwave Theory and Techniques*, vol. 39, NO. 3, March 1991.

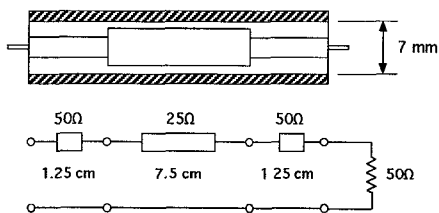


Fig. 1a. 7 mm Beatty Standard terminated in a matched load.

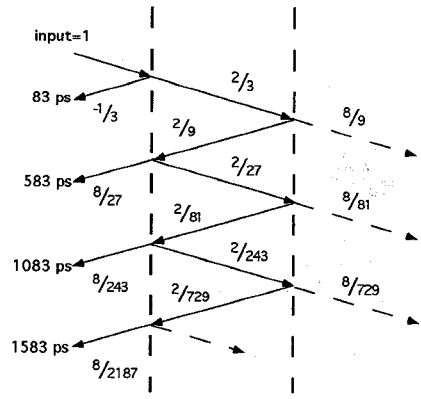


Fig. 1b. Beatty Standard bounce diagram with unit impulse stimulus.

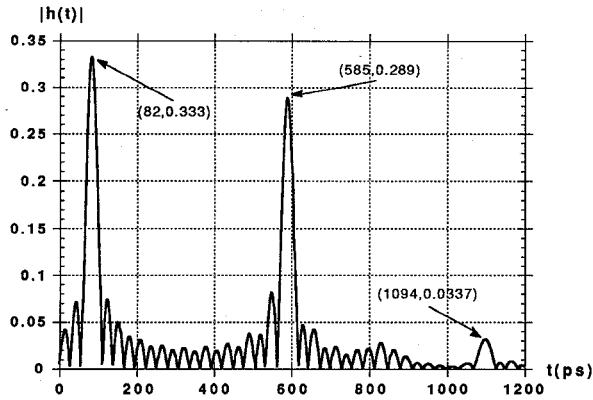


Fig. 2. Inverse FFT of 801 measurements of the reflection coefficient at the input port of the 7 mm Beatty Standard. The bandwidth used in this measurement is 18 GHz.

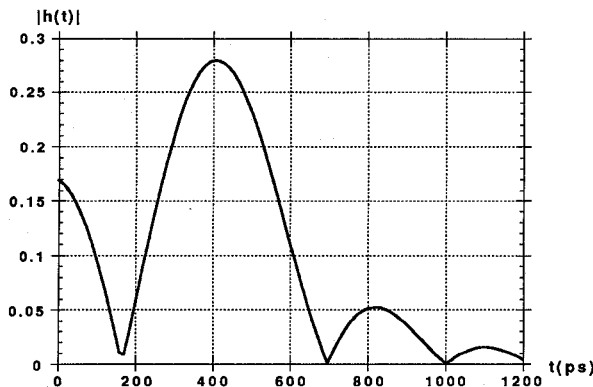


Fig. 3. Inverse FFT of 801 measurements of the reflection coefficient at the input port of the 7 mm Beatty Standard. The bandwidth used in this measurement is 2 GHz.

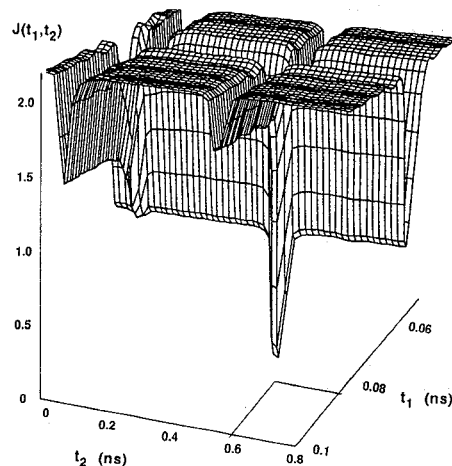


Fig. 4. Amplitude optimized objective function constructed from 801 reflection coefficient measurements of the 7 mm Beatty Standard using a bandwidth of 18 GHz.

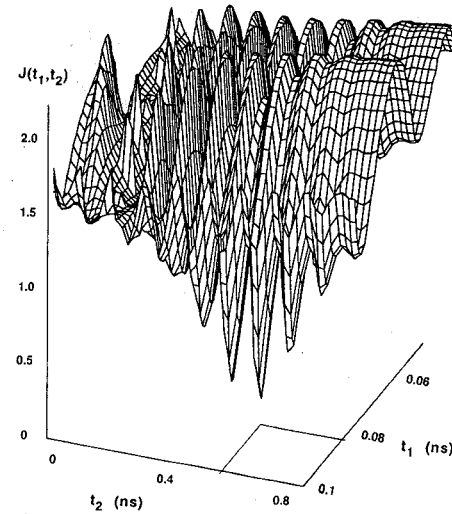


Fig. 5. Amplitude optimized objective function constructed from 801 reflection coefficient measurements of the 7 mm Beatty Standard using a bandwidth of 2 GHz.

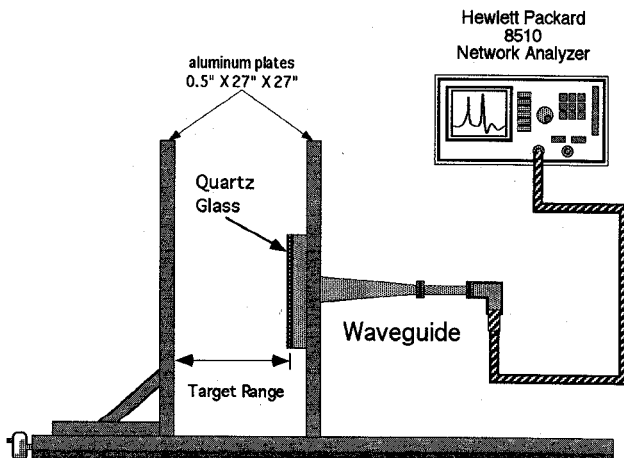


Fig. 6. Microwave reflectometer test apparatus.

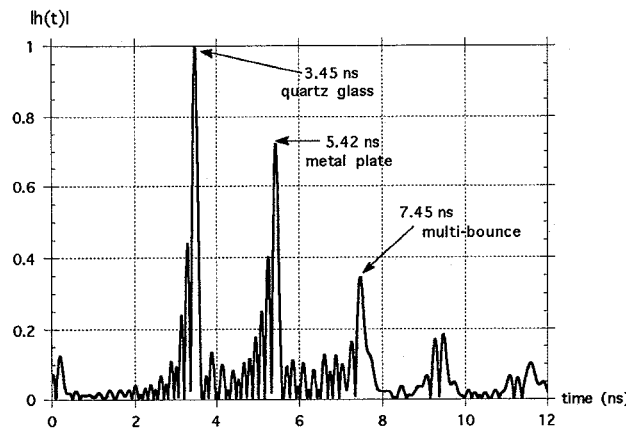


Fig. 7. Normalized Inverse FFT of 801 measurements of the reflection coefficient at the input port of the test apparatus. The bandwidth used in this measurement is 4 GHz, and the target range is 12.125".

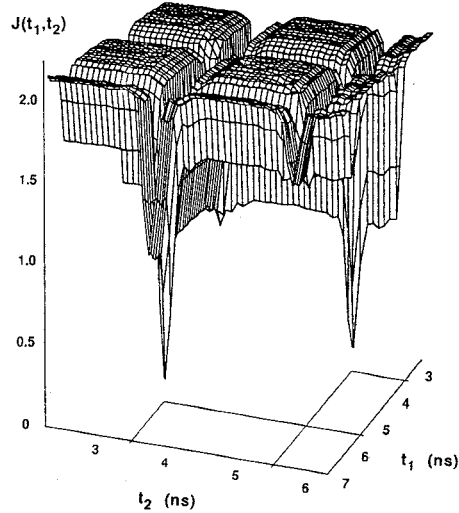


Fig. 8. Amplitude optimized objective function constructed from 801 reflection coefficient measurements of the test apparatus using a bandwidth of 4 GHz. The target range is 12.125".

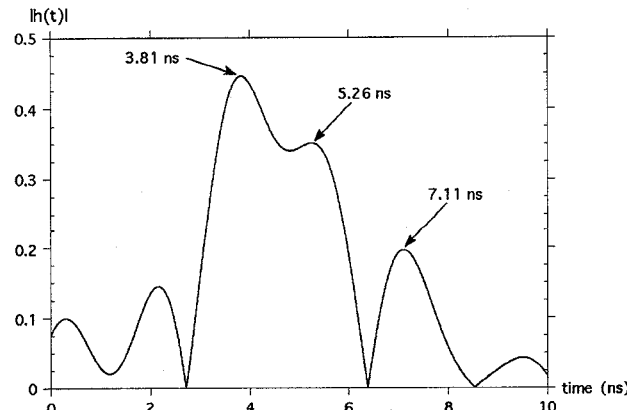


Fig. 9. Normalized Inverse FFT of 101 measurements of the reflection coefficient at the input port of the test apparatus. The bandwidth used in this measurement is 500 MHz, and the target range is 12.125".

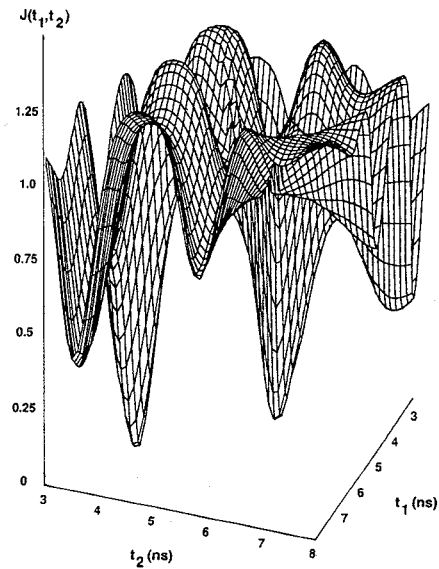


Fig. 10. Amplitude optimized objective function constructed from 101 reflection coefficient measurements of the test apparatus using a bandwidth of 500 MHz. The target range is 12.125".

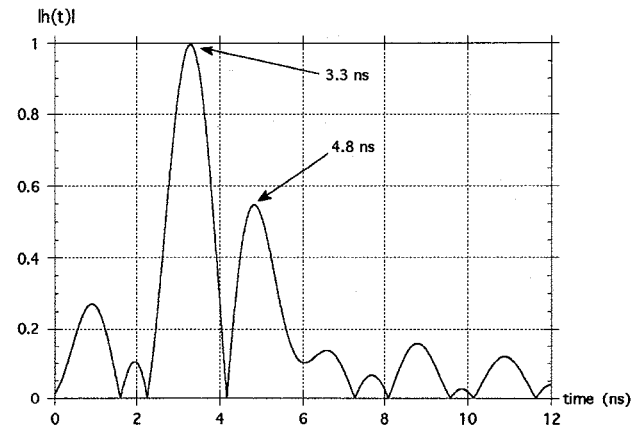


Fig. 11. Normalized Inverse FFT of 101 measurements of the reflection coefficient at the input port of the test apparatus. The bandwidth used in this measurement is 500 MHz, and the target range is 2.375".

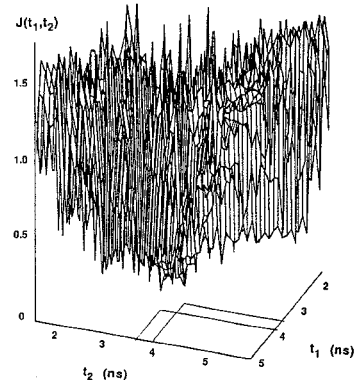


Fig. 12. Amplitude optimized objective function constructed from 101 reflection coefficient measurements of the test apparatus using a bandwidth of 500 MHz. The target range is 2.375".